This article has been accepted for publication in a future issue of this journal, but has not been fully edited. Content may change prior to final publication. Citation information: DOI 10.1109/TAP.2019.2957116, IEEE Transactions on Antennas and Propagation

The Impact of Rain on Short E-band Radio Links for 5G Mobile Systems: Experimental Results and Prediction Models

Lorenzo Luini, *Senior Member, IEEE*, Giuseppe Roveda, Maurizio Zaffaroni, Mario Costa, Carlo Riva, *Senior Member, IEEE*

***Abstract* — Results from one year of data collected during an electromagnetic wave propagation experiment at E band are presented. The research activity originates from the collaboration between Politecnico di Milano and the Huawei European Microwave Centre in Milan, which installed short (325 m) terrestrial links operating at 73 and 83 GHz, connecting two buildings in the university main campus. The received power data are processed, using a novel approach, to identify rain events and to remove the wet antenna effect, with the aim of accurately quantifying the fade induced by precipitation, A_R. Moreover, A_R is estimated by taking advantage of the ancillary data collected by the laser-based disdrometer collocated with the link transceivers. Results definitely point out the higher prediction accuracy achieved by exploiting the information on the rain drop size. A full year of data are used as reference to test the accuracy of the statistical prediction model for terrestrial links currently recommended by the ITU-R, which reveals a large overestimation. Finally, alternative models providing a higher accuracy are proposed and their accuracy assessed.**

***Index Terms* — Electromagnetic wave propagation, measurement, terrestrial links, 5G mobile networks.**

I. Introduction

The constant increase in data rate and traffic demand for wireless communication systems calls for the use of a larger bandwidth and, hence, of higher frequency bands [1]. While the 4G cellular communication system is reaching maturity in most of the Countries, the implementation of the 5th Generation (5G) has already started and will guarantee much higher data rates by using the millimeter-wave portion of the spectrum, both for backhauling links and radio access [2].

Although the use of higher carrier frequencies brings clear advantages in terms of available bandwidth and of more compact equipment, the strong impairments to the propagation of electromagnetic (EM) waves, induced by suspended water droplets (namely fog for terrestrial links), gases (oxygen and water vapor) and hydrometeors (e.g. rain, snow, hail, …) [3] must be considered for the frequency bands envisaged for 5G systems (typically from 26 GHz up to even the optical range). Among such impairments, precipitation plays the most relevant role because of the absorption and scattering caused by rain drops at frequencies higher than 10 GHz. Therefore, it is crucial to investigate rain attenuation and its dependence on the operational frequency, as well as on the rain drop dimension, i.e. on the so called Drop Size Distribution (DSD). Propagation experiments are key to support the research activities aiming to investigate the basic physical mechanisms of interaction between EM waves and hydrometeors, which, in turn, is the first necessary step to develop models for the prediction of rain attenuation statistics affecting terrestrial links, including the very short ones to be soon employed in 5G systems.

Several methods have been proposed in the past to predict statistics of rain attenuation along terrestrial links. The main input information, common to all the prediction methodologies, is the point rainfall rate, either associated just to a single exceedance probability [4] or to the full statistical distribution [5]. Some physically based methodologies assume that the link is crossed by single cells of different shape (e.g. cylindrical or exponential [6]) and given probability of occurrence. Other methods propose a simpler approach based on the calculation of the specific rain attenuation due to rain multiplied by the path length L, properly adjusted by a reduction factor that takes into account the spatial inhomogeneity of the precipitation along the link [7], [8], [4], [5]. Though some of these models provide a good prediction accuracy, they have been developed and/or tuned on the basis of experimental data collected mostly using long links (i.e. $L > 10$ km) and frequencies lower than 30 GHz: indeed, dedicated propagation experiments are needed to evaluate the accuracy of the available prediction models in predicting rain attenuation along the short high-frequency links for 5G mobile systems.

This contribution presents the results from one year of data (from February 2017 to January 2018) collected using terrestrial radio links, in the frame of a joint research activity on EM wave propagation involving Politecnico di Milano and the Huawei European Microwave Centre in Milan. The propagation campaign, which was preliminary described in [9], takes advantage of two 325-m links operating in the E band (73

Manuscript received XXXX.

Lorenzo Luini and Carlo Riva are with the Dipartimento di Elettronica, Informazione e Bioingegneria, Politecnico di Milano, Piazza Leonardo da Vinci, 32, 20133, Milano, Italy, and with the Istituto di Elettronica e di Ingegneria dell'Informazione e delle Telecomunicazioni (IEIIT), Consiglio Nazionale delle Ricerche, Via Ponzio 34/5, Milano 20133, Italy (e-mail: lorenzo.luini@polimi.it).

Giuseppe Roveda, Maurizio Zaffaroni, Mario Costa are with Huawei Microwave Centre, Segrate (MI) 20090, Italy.

0018-926X (c) 2019 IEEE. Personal use is permitted, but republication/redistribution requires IEEE permission. See http://www.ieee.org/publications_standards/publications/rights/index.html for more information.

This article has been accepted for publication in a future issue of this journal, but has not been fully edited. Content may change prior to final publication. Citation information: DOI 10.1109/TAP.2019.2957116, IEEE Transactions on Antennas and Propagation

and 83 GHz). The transceiver is a current Huawei commercial product.

The total tropospheric attenuation is first derived from the received power using a processing approach that relies on using as reference the attenuation due to gases, in turn estimated from collocated meteorological measurements. Afterwards, rain attenuation is isolated by taking advantage of the precipitation data collected by the collocated disdrometer, and the effect induced by the water persisting on the antenna surface is also investigated and removed from the measurements. A full year of data are used as reference to test the accuracy of some statistical prediction models aiming to predict rain attenuation affecting terrestrial links, including the one currently recommended by the ITU-R [4].

The remainder of this contribution is structured as follows. Section II describes the system architecture, the measurement equipment and the propagation data collected in the frame of the experiment. Section III describes the data processing and Section IV is focused on rain attenuation, which is extracted from the link measurements and estimated by taking advantage of the ancillary data collected by the disdrometer. Section V shows the results of the rain attenuation statistical analysis, while Section VI is devoted to testing the prediction models against the measured rain attenuation statistics. Finally, Section VII draws some conclusions.

II. System Architecture and Experimental Data

A. Huawei E-band Terrestrial Links

Fig. 1 shows the Huawei E-band radio transceivers installed on the rooftop of Building 20 of Politecnico di Milano (left side). The right side of the same figure shows the link path connecting Buildings 14 and 20 in the main university campus, whose length, L, is equal to 325 m.

Fig. 1. The E-band Huawei link transceiver (left side) and the corresponding link path between Buildings 14 and 20 of Politecnico di Milano (right side).

The E-band system covers the 71-86 GHz frequency range, with a channel bandwidth of 250 MHz. As further detailed in Fig. 2, which depicts the experiment architecture, two 250-MHz channels are used with Frequency Division Duplexing (FDD), on carrier frequencies of 73 GHz ("Low" band, transmitted from Building 20 to Building 14) and 83 GHz ("High" band, transmitted from Building 14 to Building 20). The Received Signal Level (RSL) in dBm (both channels) is sampled every 0.05 seconds (20 samples per second). The data are stored on a PC installed in a room of Building 20; the connection from the PC to the radio units is achieved by means of an Ethernet cable for building 20, and by means of an additional radio control channel for building 14. The application on the PC monitors the registers inside the radio units where the RSL data are stored.

Both links share a common antenna for the TX and the RX, which includes a duplexer; the main system parameters are summarized in Table I. Over a distance of 325 m, the resulting atmospheric fade margin is of approximately 36 dB, sufficient to properly assess the impact of precipitation on the links. The baseband subsystem can operate with M-QAM (M-ary Quadrature Amplitude Modulation) modulation (up to 256 QAM), but the link is operated with QPSK (Quadrature Phase Shift Keying) modulation, in order to maximize the signal-to-noise ratio (SNR), hence the atmospheric fade margin.

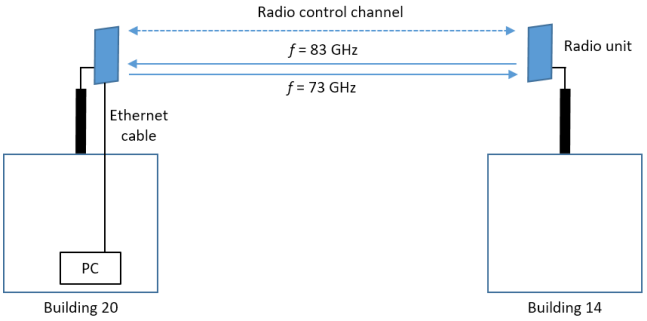

Fig. 2. Experiment architecture.

TABLE I. Main System Parameters of the E-band Links.

Channel bandwidth	250 MHz
Transmitter power	+ 10 dBm
Receiver sensitivity	-71 dBm with QPSK
Antenna gain (both TX and RX)	40 dBi
Wave polarization	Linear vertical
Carrier frequencies	73 GHz (Low) 83 GHz (High)
Atmospheric fade margin	36 dB

B. Thies CLIMA Laser Disdrometer

Among the ancillary instruments installed on the rooftop of the Building 20 of Politecnico di Milano, the Thies CLIMA Laser Precipitation Monitor (or disdrometer), pictured in Fig. 3, is located alongside the Huawei link transceivers. It operates by means of an infrared laser diode, which generates a 785-nm beam over an area of 4560 mm^2 [10]. A photodiode receiver monitors fluctuations in the received signal power as precipitating particles cross the beam. Using this information, the particle diameter is derived from the magnitude of the signal attenuation. The observed particles are classified into spectra of 22 diameter bins from 0.125 mm to 8 mm with non-uniform bin widths [10]. Through on-board processing, the instrument also classifies the type of precipitation (e.g. rain, snow, hail, …) and

0018-926X (c) 2019 IEEE. Personal use is permitted, but republication/redistribution requires IEEE permission. See http://www.ieee.org/publications_standards/publications/rights/index.html for more information.

This article has been accepted for publication in a future issue of this journal, but has not been fully edited. Content may change prior to final publication. Citation information: DOI 10.1109/TAP.2019.2957116, IEEE Transactions on Antennas and Propagation

calculates rain intensity. Measurements are recorded with 1-minute integration time.

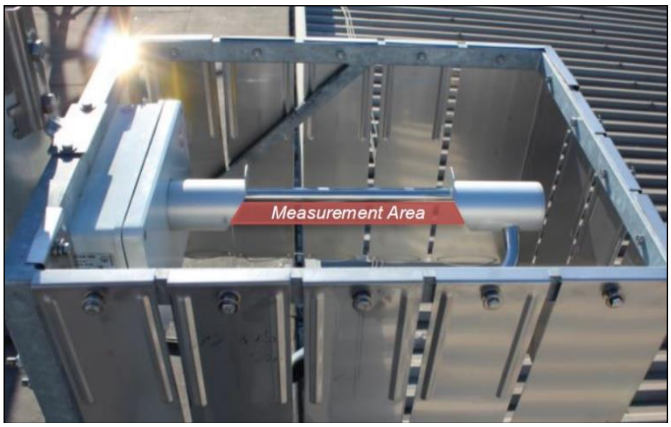

Fig. 3. The Thies CLIMA Laser disdrometer installed on the rooftop of Building 20 of Politecnico di Milano campus.

C. The Meteorological Sensors

Installed on the rooftop of Building 20, in the frame of a satellite propagation experiment [11], the RPG-LWP+72.5/82.5-GHz radiometer measures the natural sky EM emissions (brightness temperature) in four channels around 23.8, 31.6, 72.5 and 82.5 GHz. Of specific interest for the Huawei/PoliMi propagation experiment are the meteorological sensors installed on the radiometer, which sample, each second, the ground pressure, temperature, relative humidity, wind direction and intensity, and the occurrence of rain: in fact, as explained in detail in Section III.B, this information is key to derive the path attenuation due to gases affecting the E-band terrestrial links.

III. Data Processing

A. Pre-processing

The RSL collected by the link transceivers are centralized to the Huawei PC installed at Politecnico di Milano. Raw data files are retrieved remotely by Huawei to apply the following pre-processing steps:

- The time stamps of the samples are accurately synchronized (Coordinated Universal Time – UTC).
- Signal spikes are filtered out.

Afterwards, the pre-processed data are made available to Politecnico di Milano for the investigation and quantification of the effects induced by the tropospheric constituents on the links. To this purpose, considering the integration time of the disdrometer and the aim to relate the rain rate data with the received power, all the data collected by the Huawei transceivers are averaged over 1 minute. As an example, Fig. 4 shows the signal level received by the E-band link at 83 GHz, P_{RX}, on the 13th of May 2017, both with the original sampling time and after applying the 1-minute average. As is clear from the sudden drop of P_{RX} (more than 5 dB), a strong rain event affected the link between 14 and 16 UTC, while some precipitation with moderate intensity is also visible at the end of the day.

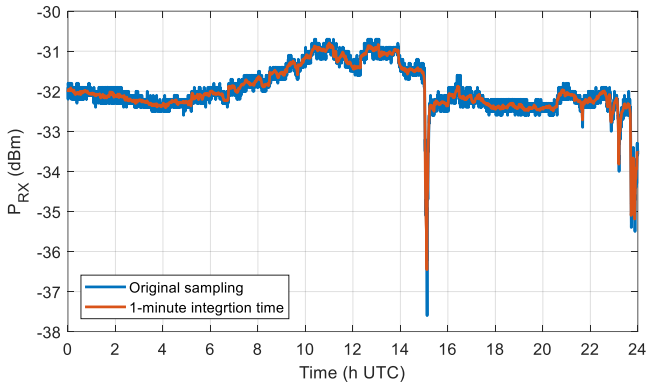

Fig. 4. Signal level received by the E-band link (f = 83 GHz), P_{RX}, on the 13th of May 2017, both with the original sampling time and after applying the 1-minute average.

The collection of propagation data started in November 2016, but hardware adjustments were progressively performed to gradually optimize the system in order to increase the dynamic range. No changes have been applied to the equipment since the beginning of February 2017, which is therefore considered as the starting month for the collection of reliable propagation data.

B. Total Tropospheric Attenuation

The main purpose of propagation experiments is to assess the impact of the atmospheric constituents on electromagnetic waves, notably the one induced by rain. In this work the rain attenuation A_R is extracted from P_{RX} by using a novel approach relying, as a first step, on the calculation of the total tropospheric attenuation A_T (i.e. due to gases and rain).

In principle, A_T could be inferred from the knowledge of all the elements involved in the link budget (e.g. path length, frequency, gain of the antennas, …); in practice, the estimation of some of these quantities is hardly accurate, due to, for example, oscillations in the nominal transmitted power, changes in the gain/attenuation levels in the electronic components, possible small pointing errors, etc. A viable approach to derive A_T from P_{RX} is to exploit the ancillary information provided by the meteorological sensors collocated with the link transceivers. In fact, the pressure P, temperature T and relative humidity RH are sufficient information to accurately calculate the path attenuation due to oxygen (A_{OX}) and to water vapor (A_{WV}) using the model included in recommendation ITU-R P.676-11 (Annex 1) [12]: in rain-free conditions, and without fog (extremely rare in Milan in the last 5 years), A_T coincides with the gaseous attenuation $A_G = A_{OX} + A_{WV}$, which, estimated from the meteorological sensors, can thus be used as the reference to derive A_T from P_{RX}.

As an example, Fig. 5 shows the trend of the attenuation due to gases A_G at 83 GHz calculated using the model in Annex 1 of recommendation ITU-R P.676-11 (13th of May 2017). As expected, far from the oxygen absorption peak centered around 60 GHz [13], A_{WV} prevails over A_{OX}. It is worth noticing that during the rain event taking place between 14 and 16 UTC (see Fig. 4), both A_{WV} and A_{OX} slightly increase: this, in turn, is associated to the increase in the water vapor concentration (to which A_{WV} is positively correlated [14]) and to the decrease in

0018-926X (c) 2019 IEEE. Personal use is permitted, but republication/redistribution requires IEEE permission. See http://www.ieee.org/publications_standards/publications/rights/index.html for more information.

This article has been accepted for publication in a future issue of this journal, but has not been fully edited. Content may change prior to final publication. Citation information: DOI 10.1109/TAP.2019.2957116, IEEE Transactions on Antennas and Propagation

the temperature (to which A_{OX} is negatively correlated [13]), which typically occur during rain events.

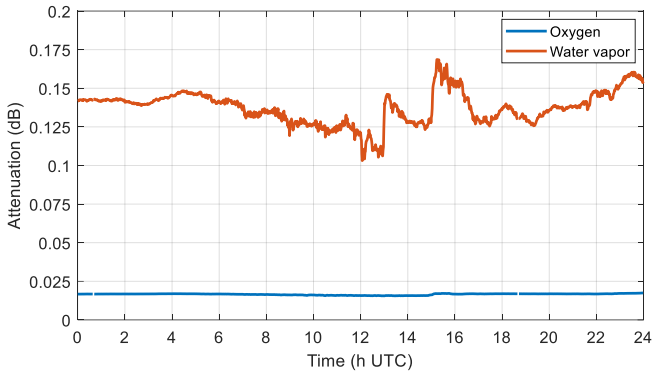

Fig. 5. A_G estimated from local measurements of P, T and RH using the model in Annex 1 of recommendation ITU-R P.676-11 (13th of May 2017); E-band link at 83 GHz.

As explained more in detail below, a key step to derive A_T from P_{RX} is to identify and isolate rain events. Given the very short path length (L = 325 m), as also verified by visual inspection of the data, rain always affects both the links and the disdrometer at the same time, such that the latter is sufficient to identify P_{RX} rainy samples. More in detail, only rain rate values higher than 0.05 mm/h are considered because of the limited statistical reliability of the disdrometer measurements for lower values. Moreover, two distinct rain events are supposed to be separated by at least 60 dry minutes. This is shown in Fig. 6, which depicts the rain rate measured by the disdrometer and the identification of two rain events occurring on the 3rd of January 2017.

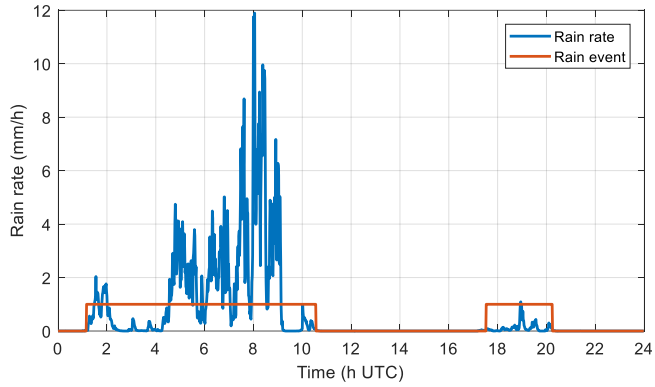

Fig. 6. Identification of rain events on the 3rd of January 2017.

From the knowledge of A_G and the identification of the rain events, the total tropospheric attenuation A_T is derived from P_{RX}. The rationale of the method, drawn from ideas applied in the context of satellite propagation experiments [15],[16], is to isolate from P_{RX} the component received power ascribable only to gases. The difference between such component and A_G is the 'correction factor' A_D to be subtracted from -P_{RX} to calculate A_T (see step 3 below). Specifically, this is achieved through the following steps:

1. Define P'_{RX} in absence of rain, $P'_{RX} = P_{RX}$, while during the rain event, P'_{RX} is calculated as the linear interpolation between the P^b_{RX} and P^a_{RX}, respectively defined as the last sample of P_{RX} before the rain event and the first sample of P_{RX} after the rain event.
2. Calculate P''_{RX} by low-pass filtering P'_{RX} to remove the fast oscillations of the signal.
3. Calculate:

$$A_D = -P''_{RX} - A_G \quad (1)$$

4. Calculate the link-derived total tropospheric attenuation A_T as:

$$A_T = -P_{RX} - A_D \quad (2)$$

The steps above are clarified in Fig. 7, which shows P_{RX}, P'_{RX} and P''_{RX} at 83 GHz for the 13th of May 2017. Also reported in the figure is the identified rain event. The final step of the calibration procedure, i.e. the application of (2), is reported in Fig. 8, which also includes the reference signal A_G. As is clear by comparing Fig. 7 and Fig. 8, the procedure outlined above allows preserving the information on the contribution of all the tropospheric constituents to the total attenuation (see for example the A_T peak just after 15 UTC) and, at the same time, to reduce the daily slow system-induced fluctuations of P_{RX}.

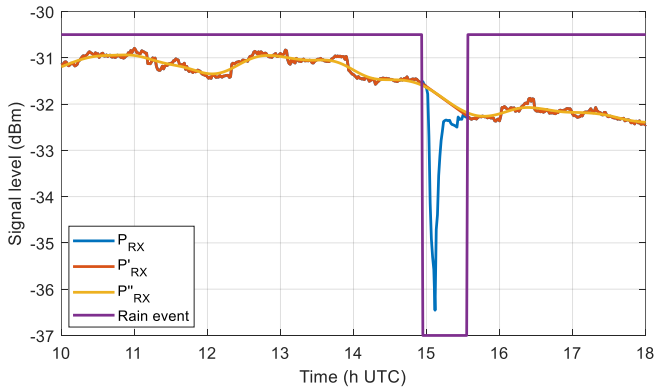

Fig. 7. Time series of P_{RX}, P'_{RX} and P''_{RX} at 83 GHz for the 13th of May 2017.

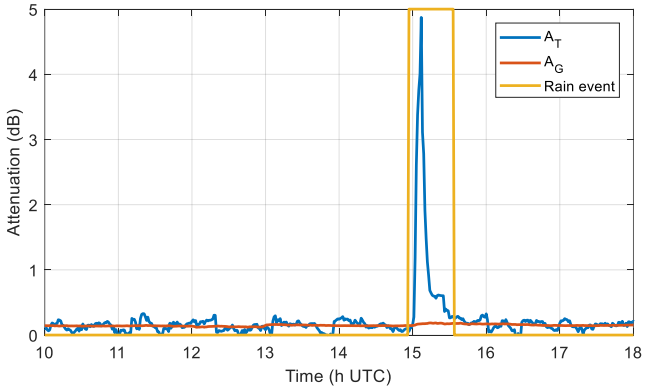

Fig. 8. Time series of the total attenuation A_T derived from P_{RX} and of the reference gaseous attenuation A_G derived from the meteorological sensors (13th of May 2017, f = 83 GHz).

0018-926X (c) 2019 IEEE. Personal use is permitted, but republication/redistribution requires IEEE permission. See http://www.ieee.org/publications_standards/publications/rights/index.html for more information.

This article has been accepted for publication in a future issue of this journal, but has not been fully edited. Content may change prior to final publication. Citation information: DOI 10.1109/TAP.2019.2957116, IEEE Transactions on Antennas and Propagation

The rain attenuation A_R is calculated as:

$$A_R = A_T - A_G \tag{3}$$

Finally, all A_R values outside the identified rain events are set to zero: Fig. 9 depicts A_R associated to the first rain event reported in Fig. 4, occurring around 15 UTC.

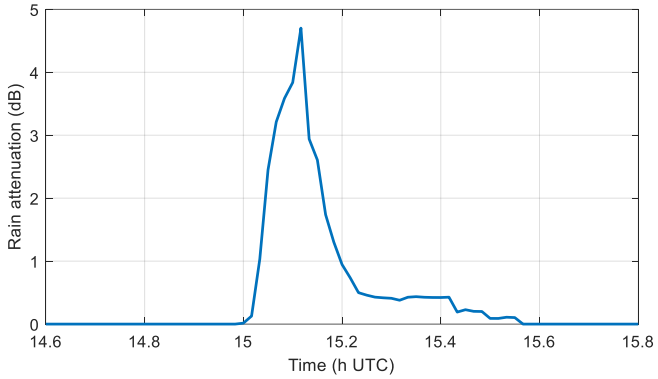

Fig. 9. Time series of the rain attenuation A_R at 83 GHz (13th of May 2017).

IV. Rain Attenuation Prediction

The disdrometer installed at short distance from the Huawei transceivers is a key resource to further investigate the effects of rain on the experimental links. In fact, the information on the rain rate, and even more, on the DSD, allows predicting the attenuation induced by rain on the links. Specifically, A_R is estimated using the two different approaches detailed hereinafter.

A. Method Based on Recommendation ITU-R P.838-3

ITU-R provides in Recommendation P.838-3 [17] simple analytical formulations to calculate the specific attenuation due to rain, γ_R. By using this model, the rain attenuation suffered from the link can be calculated as:

$$A_R^{ITU-R} = \gamma_R^{ITU-R} L = kR^{\alpha} L \tag{4}$$

k and α are the coefficients, provided in [17], that depend on the operational frequency f, the wave polarization (linear vertical for the links) and link elevation θ (0° for the links). A_R is calculated in (4) as the simple multiplication of the specific attenuation γ_R and of the link length L, assuming a constant rain rate along the path (given its short path). This assumption will be further discussed in the remainder of the paper.

B. Method Based on Disdrometric Data

The attenuation induced by rain on electromagnetic waves is not only function of the precipitation intensity R, but also of the shape and size of the rain drops [18]. This information is typically provided in terms of the DSD, which is calculated from the available disdrometric data as:

$$N(D_i) = \frac{10^6 n_i}{S\, v(D_i)\, T\, \Delta D_i} \quad (\text{mm}^{-1}\,\text{m}^{-3}) \tag{5}$$

In (5), n_i is the number of raindrops whose diameter falls in the i-th class (with mean diameter D_i), ΔD_i (mm) represents the width of each drop-size class, S (mm^2) is the disdrometer sampling area, T (seconds) is the instrument integration time, and $v(D_i)$ (m/s) is the terminal velocity of rain drops.

The specific attenuation γ_R (dB/km) at frequency f, for the drop density distribution $N(D)$, is the following function of the wavelength λ and of the forward scattering coefficient S_0 [19]:

$$\gamma_R^{DSD} = 4.343 \cdot 10^3 \frac{\lambda^2}{\pi} \sum_{i=1}^{N_c} \text{Re}\left[S_0(D_i, f)\right] N(D_i) \Delta D_i \tag{6}$$

The forward scattering coefficient S_0 is calculated using the T-matrix approach [20], assuming the axial ratio defined by Beard and Chuang [21]. Finally:

$$A_R^{DSD} = \gamma_R^{DSD} L \tag{7}$$

Like for the ITU-R based method, the rain rate is assumed to be constant along the path.

C. Prediction Results

Fig. 10 gives a hint of the accuracy of the two methods outlined above in predicting rain attenuation starting from the ancillary information provided by the disdrometer. In the figure, the blue line represents the rain attenuation time series measured by the links, while the red dashed and the black dashed lines are the prediction based on recommendation ITU-R P.838-3, and on the measured DSD data, respectively. Results refer to the rain event occurring on the 13th of May 2017 at 83 GHz. Fig. 11 shows the corresponding rain rate time series.

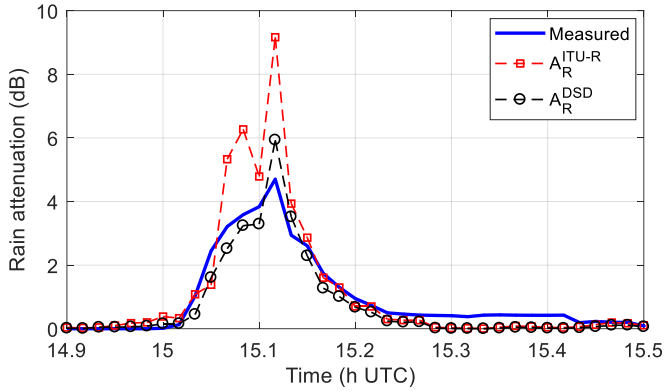

Fig. 10. Rain attenuation at 83 GHz on the 13th of May 2017, derived from the link (blue line), estimated from R using recommendation ITU-R P.838-3 (red dashed line with squares) and estimated from DSD data (black dashed line with circles).

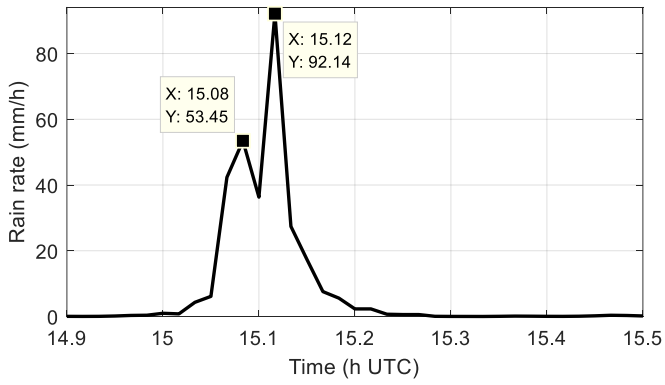

0018-926X (c) 2019 IEEE. Personal use is permitted, but republication/redistribution requires IEEE permission. See http://www.ieee.org/publications_standards/publications/rights/index.html for more information.

This article has been accepted for publication in a future issue of this journal, but has not been fully edited. Content may change prior to final publication. Citation information: DOI 10.1109/TAP.2019.2957116, IEEE Transactions on Antennas and Propagation

Fig. 11. Measured rain rate (13th of May 2017).

The two approaches described above to predict A_R provide quite different results: the trend of the three curves is similar, but A_R^{DSD} clearly offers a much better estimate than A_R^{ITU-R}. More in detail, it is worth pointing out how the peak rain rate of approximately 53 mm/h (see Fig. 11) has actually much more limited impact on the link than what is predicted using the ITU-R approach: notwithstanding the high rain intensity, A_R is lower than 4 dB, while A_R^{ITU-R} exceeds 6 dB. On the other hand, A_R is well estimated by A_R^{DSD}, which, differently from A_R^{ITU-R}, takes advantage of the information on the DSD. Indeed, especially at high frequency, small (e.g. D around 0.5 mm) and large (e.g. D around 3 mm) drops definitely have a different impact on electromagnetic waves. More specifically, even a few large drops significantly contribute to the increase in R, while they have a more limited impact on A_R^{DSD}: in fact, while R depends on cube of D [18], the forward scattering coefficients in (6) depends on the square of the drop diameter [20].

Similar results are obtained for the second high rain intensity peak reported in Fig. 11 (roughly 90 mm/h): though both approaches overestimate the rain attenuation measured by the link, A_R^{DSD} is once again more accurate.

The key role of the DSD in the calculation of rain attenuation is confirmed by the additional results shown in Fig. 12, which reports the measured and estimated rain attenuation on the 26th of April 2017 at 73 GHz. The rain rate for the same day is depicted in Fig. 13. It is interesting to notice that, while in Fig. 10 A_R^{DSD} is lower than A_R^{ITU-R}, in this second example, A_R^{DSD} exceeds A_R^{ITU-R}, yet still providing the best prediction accuracy.

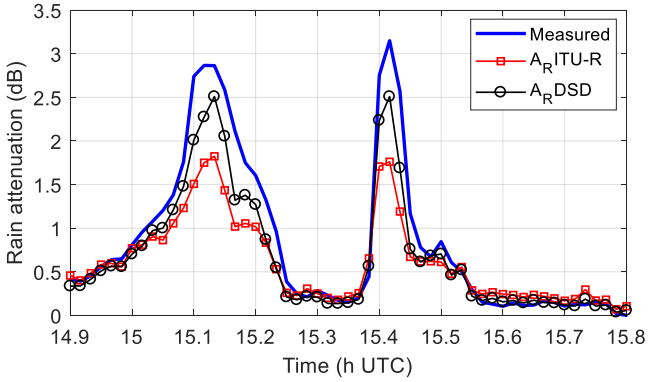

Fig. 12. Rain attenuation at 73 GHz on the 26th of April 2017, derived from the link (blue line), estimated from R using recommendation ITU-R P.838-3 (red dashed line with squares) and estimated from DSD data (black dashed line with circles).

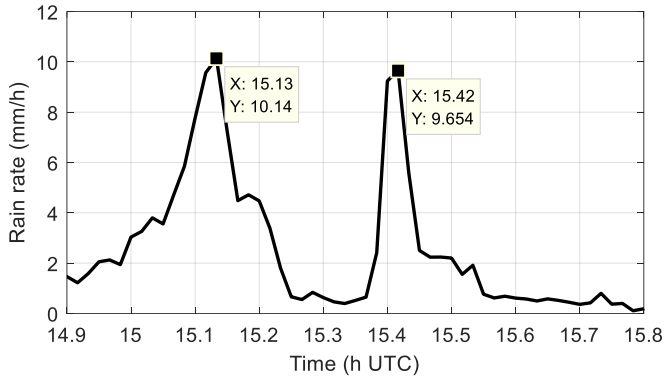

Fig. 13. Measured rain rate (26th of April 2017).

D. Wet Antenna Correction

As is clear from Fig. 10 and Fig. 12, overall, A_R^{DSD} tends to be lower than A_R: this is likely due to the wet antenna effect impairing both links, which is investigated in this section.

Hong et al. [22] clearly points out the wet antenna issue affecting the measurements performed with a long V- and W-band terrestrial link in Albuquerque, New Mexico, USA: the authors show that the wet antenna problem can be significantly mitigated by using an antenna radome treated with a hydrophobic coating. However, no model is proposed to remove the wet antenna induced attenuation from the measurements. This is done in [23], where the signal received in Vancouver, Canada, from the ACTS satellite is processed to isolate and study the wet antenna effect. The authors define a simple yet effective model for wet antenna correction:

$$A'_R = A_R - A_{WA} = A_R - a\left(1 - e^{-bA_R}\right) \quad (8)$$

where A_R is the rain attenuation estimated from the received power using the procedure outlined in Section III.B, A_{WA} is the attenuation induced by the wet antenna and A'_R is the actual rain attenuation. According to (8), A_{WA} increases with A_R (i.e. with the rain rate R) and reaches a maximum constant value a. In [23], a = 2.62 dB and b = 0.52 dB^{-1}, but obviously these coefficients are strongly dependent on the system parameters, mainly on the frequency, and the type of antenna/radome and coating. The same model in (8) was used (and modified to express A_{WA} as a function of the estimated path attenuation) with different coefficients in [24] to remove the wet antenna contribution from propagation measurements collected at W band using terrestrial links with a path length of 840 m.

In this work, the wet antenna attenuation contribution is estimated by taking advantage of the available disdrometer data. The proposed approach compares the specific attenuation γ_T, obtained by dividing the measured link attenuation A_L by the path length L, and the specific attenuation γ_R^{DSD}, calculated from DSD data according to (6). However, this comparison is sensible only considering stratiform rain events, which typically occur during winter in Milan. In fact, for such events, the assumption that the rain rate (and the DSD) is constant along the whole link, which underpins the calculation of $\gamma_T = A_L/L$, is most probably valid, while it becomes more and more questionable as the rain rate increases, i.e. during convective

0018-926X (c) 2019 IEEE. Personal use is permitted, but republication/redistribution requires IEEE permission. See http://www.ieee.org/publications_standards/publications/rights/index.html for more information.

This article has been accepted for publication in a future issue of this journal, but has not been fully edited. Content may change prior to final publication. Citation information: DOI 10.1109/TAP.2019.2957116, IEEE Transactions on Antennas and Propagation

events. Indeed, in this case, rain cells tend to become smaller and smaller, and the rain rate varies along the link [25].

Fig. 14 shows the specific attenuations γ_T and γ_R^{DSD}, as a function of the rain rate R obtained from the DSD data: only stratiform events relative to February 2017 and to the period from November 2017 to January 2018 are considered. Fig. 14 also reports the power law ($\gamma = k\,R^{\alpha}$) fitting both data sets. For the sake of comparison, also the values extracted from recommendation ITU-R P.838-3 are added to Fig. 14 [17]. Table II lists all the values of k and α for both links at 73 and 83 GHz.

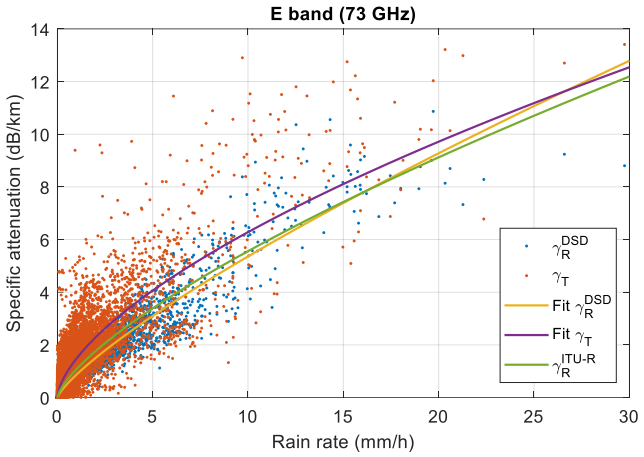

Fig. 14. Specific attenuation (derived from the link and from the DSD data) as a function of the rain rate (obtained from DSD data), for the link at 73 GHz. Only stratiform events considered: February 2017, and from November 2017 to January 2018 (included).

Based on the results in Fig. 14, the attenuation induced by the wet antenna is estimated as follows:

$$A_{WA} = \left[k^{L}(R)^{\alpha^{L}} - k^{DSD}(R)^{\alpha^{DSD}} \right] L \tag{9}$$

where (k^L, α^L) and (k^{DSD}, α^{DSD}) are the power law coefficients for the link data and for the DSD data, respectively, listed in Table II. Fig. 15 shows A_{WA} as a function of A_R, the latter calculated as $A_R = k^{L}(R)^{\alpha^{L}} L$.

TABLE II. POWER LAW COEFFICIENTS $\gamma = k\,R^{\alpha}$ DERIVED FROM THE LINK DATA, THE DSD DATA AND RECOMMENDATION ITU-R P.838-3. ONLY STRATIFORM EVENTS CONSIDERED: FEBRUARY 2017, AND FROM NOVEMBER 2017 TO JANUARY 2018.

	E band low (f = 73 GHz)			E band high (f = 83 GHz)		
	Link data	**DSD data**	**ITU-R P.838-3**	**Link data**	**DSD data**	**ITU-R P.838-3**
k	1.509	0.8654	1.0711	1.323	1.033	1.2034
α	0.6215	0.7918	0.7150	0.6442	0.7528	0.6973

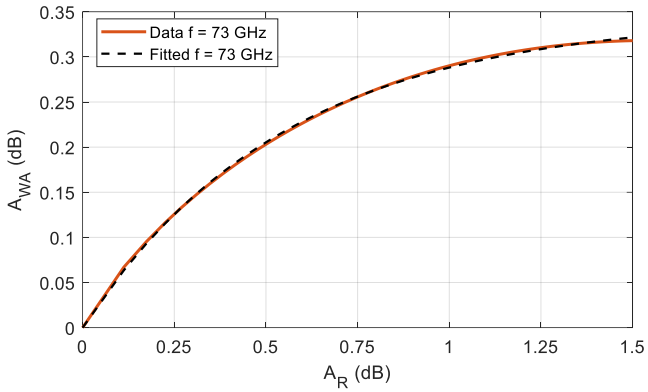

Fig. 15. Estimated A_{WA} as a function of A_R at f = 73 GHz for stratiform events.

Fig. 15 also includes the curve fitting A_{WA} (black dashed line), according to the model proposed in [23]:

$$A_{WA}^{*} = \begin{cases} 0.3528\left(1 - e^{-1.815 A_R}\right) & A_R \le 1.5\,\text{dB} \\ 0.33 & A_R > 1.5\,\text{dB} \end{cases} \tag{10}$$

As is clear from (10), the exponential expression modelling A_{WA} is considered valid up to A_R = 1.5 dB: in fact, though not shown in Fig. 15, for larger values of A_R, the trend of A_{WA} calculated through (9) becomes decreasing. This behavior is definitely unlikely, and points out the limited validity of the assumption that the rain rate is constant along the link for convective events. On the other hand, as also explained in [23], the wet antenna attenuation is expected to reach a plateau value, correctly modeled by (10), which is independent of the rain rate. Finally, it is worth noticing that, overall, the wet antenna attenuation estimated by means of the model in (10) is actually quite limited (up to 0.33 dB): indeed, as clearly shown in Fig. 7 and Fig. 8, the larger portion of A_{WA} is already removed by correctly identifying the rain events along the link and by using the reference gaseous attenuation to derive A_T from P_{RX}.

As a result, the rain attenuation is derived as $A'_R = A_R - A_{WA}^{*}$. The same methodology, applied to the 83 GHz link data, yields:

$$A_{WA}^{*} = \begin{cases} 0.1068\left(1 - e^{-4.167 A_R}\right) & A_R \le 0.7\,\text{dB} \\ 0.1 & A_R > 0.7\,\text{dB} \end{cases} \tag{11}$$

A difference in the two correction models is expected because of the dependence on frequency of the attenuation induced by the wet antenna and of the one due to the precipitation along the path.

As an example of the wet antenna correction procedure, Fig. 16 depicts a rain event occurred at 73 GHz on the 3rd of February 2017, together with the associated rain rate: the agreement between the rain attenuation estimated from the link and using the DSD data is very good.

0018-926X (c) 2019 IEEE. Personal use is permitted, but republication/redistribution requires IEEE permission. See http://www.ieee.org/publications_standards/publications/rights/index.html for more information.

This article has been accepted for publication in a future issue of this journal, but has not been fully edited. Content may change prior to final publication. Citation information: DOI 10.1109/TAP.2019.2957116, IEEE Transactions on Antennas and Propagation

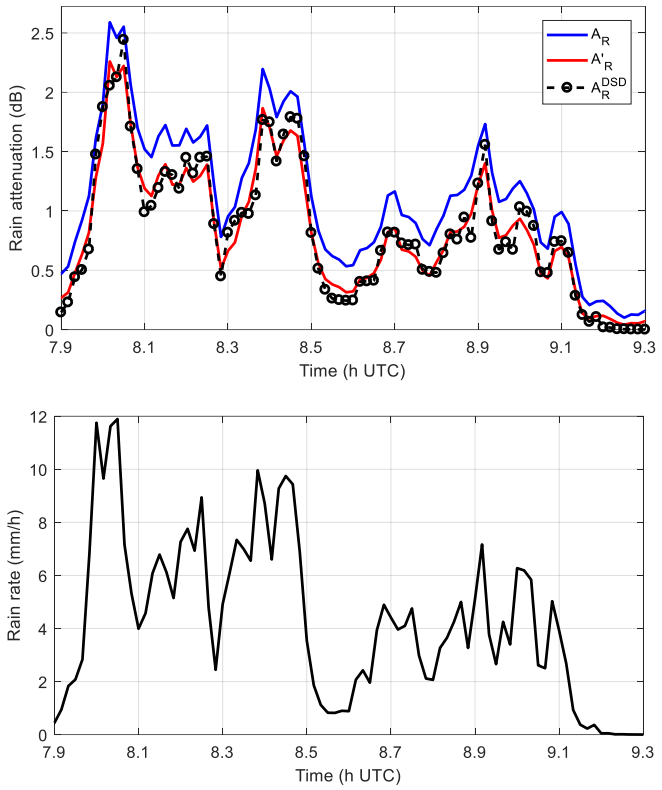

Fig. 16. Top: attenuation (73 GHz, 3rd of February 2017) A_R (blue line), A'_R (red line) and A_R^{DSD} (black dashed line with circles); bottom: concurrent rain rate.

V. Rain Attenuation Statistical Analysis

Fig. 17 and Fig. 18 show the Complementary Cumulative Distribution Functions (CCDFs) of the rain attenuation A'_R as derived from one full year of link data (from February 2017 to January 2018) and as estimated according to the procedures outlined in the previous sections. The link data availability is 97.8% and 97.6% for the low (73 GHz) and high (83 GHz) channels, respectively.

The comparison between the link data and the estimated data is more interesting: on the one side, results confirm that recommendation ITU-R P.838-3 tends to overestimate the measured data for more intense rain rates (attenuation larger than 3 dB); on the other side, the prediction achieved using the DSD data is in good agreement with the experimental curves for exceedance probabilities approximately higher than $P^* = 0.02\%$ (mostly stratiform events). For $P < P^*$ (mostly convective events), the prediction overestimates the measurements: this is likely due to the fact that the higher is the rain intensity (i.e. the rain attenuation), the more questionable is to consider a constant rain rate along the link equal to the value measured by the disdrometer: in fact, results point out that, for intense events, overall, the mean rain rate along the link is lower than the point values measured by the disdrometer. This, in turn, is a hint that the effective path reduction factor r, defined in several rain attenuation prediction models to account for the rain rate inhomogeneity along the path (e.g., Recommendation ITU-R P.530-17 [4]), is lower than 1 for the experimental links investigated in this work.

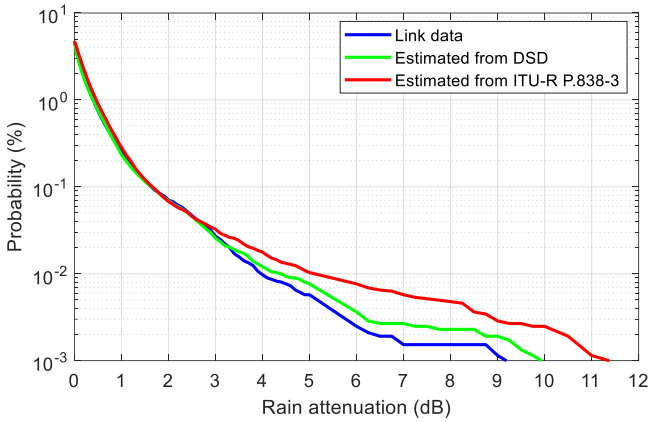

Fig. 17. CCDF of the rain attenuation (measured and estimated) at 73 GHz (one year observation period from February 2017 to January 2018).

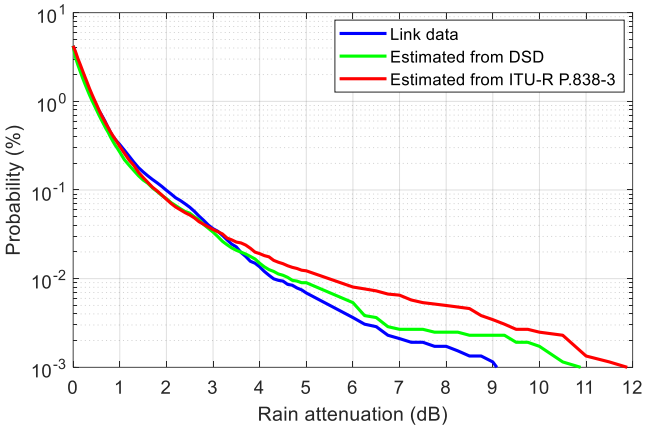

Fig. 18. CCDF of the rain attenuation (measured and estimated) at 83 GHz (one year observation period from February 2017 to January 2018).

Fig. 19 completes the statistical analysis of the rain attenuation by reporting the rain rate CCDF measured by the disdrometer in the same period (from February 2017 to January 2018): the probability to have rain is $P_0 = 4.75\%$ and the rain rate exceeded for 0.01% of the yearly time is $R_{0.01\%} = 41.9$ mm/h.

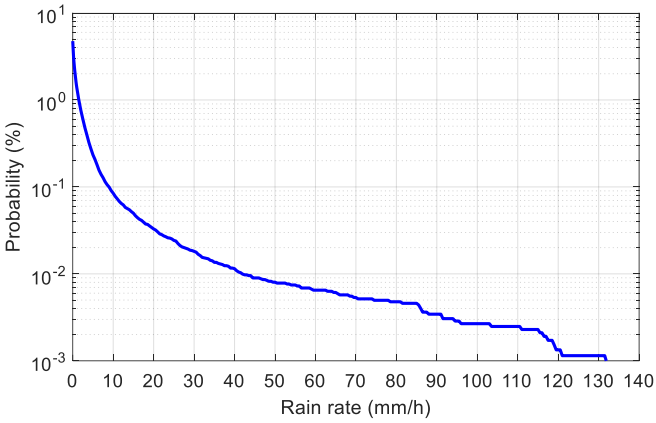

Fig. 19. CCDF of the rain rate as measured by the disdrometer in Milan in the period February 2017-January 2018.

0018-926X (c) 2019 IEEE. Personal use is permitted, but republication/redistribution requires IEEE permission. See http://www.ieee.org/publications_standards/publications/rights/index.html for more information.

This article has been accepted for publication in a future issue of this journal, but has not been fully edited. Content may change prior to final publication. Citation information: DOI 10.1109/TAP.2019.2957116, IEEE Transactions on Antennas and Propagation

VI. Prediction Model Testing

Recommendation ITU-R P.530-17 includes a methodology to estimate the rain attenuation on terrestrial links, valid for path lengths up to 60 km and frequencies lower than 100 GHz [4]. Besides the electrical and geometrical features of the link (e.g. frequency and link elevation), the model receives as input the local value of the rain rate exceeded for 0.01% of the yearly time and relies on the concept of path reduction factor r to account for the inhomogeneity of the rain rate along the link.

Fig. 20 and Fig. 21 compare the predictions obtained using Recommendation ITU-R P.530-17 with the measured data (wet antenna effect removed), for both links (f = 73 GHz and 83 GHz, respectively, one year observation period from February 2017 to January 2018). More specifically, the ITU-R model is applied by using different input values, i.e.:

- *Local inputs*: $R_{0.01\%}$ = 41.9 mm/h, as obtained from the concurrent local DSD-derived rain rate statistics (see Fig. 19); k and α as listed in Table III, calculated from DSD data as done for Fig. 14, but using the full period.
- *ITU-R derived inputs*: $R_{0.01\%}$ = 35.3 mm/h, as obtained from recommendation ITU-R P.837-7 (see Fig. 19); k and α as extracted from Recommendation ITU-R P.838-3 (see Table II).

As is clear from the prediction results, regardless of the input values, the model included in recommendation ITU-R P.530-17 largely overestimates the measured data. This is due to the very high values of the path reduction factor r, which, for the above tests, ranges between 2.34 (f = 83 GHz, local inputs) to 2.5 (f = 73 GHz, ITU-R derived inputs). In turn, such high values mainly depend on the very short path length (d = 0.325 km), as clearly shown in Fig. 22, where r is depicted as a function of the path length d (ITU-R derived inputs). Indeed, the dependence of r on the frequency is very limited, while r steeply increases to values larger than 1 for d < 2 km.

TABLE III. Power Law Coefficients $\gamma = kR^{\alpha}$ Derived from the DSD Data. Full Period Considered: from February 2017 to January 2018 (Included).

	f = 73 GHz	f = 83 GHz
k	0.9688	1.119
α	0.6901	0.6727

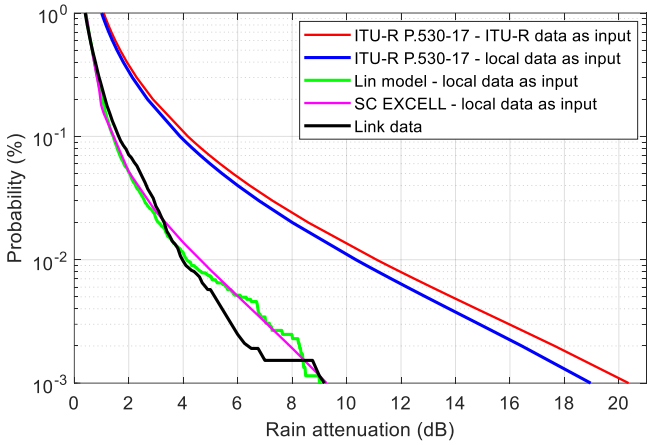

Fig. 20. Comparison between the rain attenuation CCDF measured using the link and estimated by prediction models; f = 73 GHz.

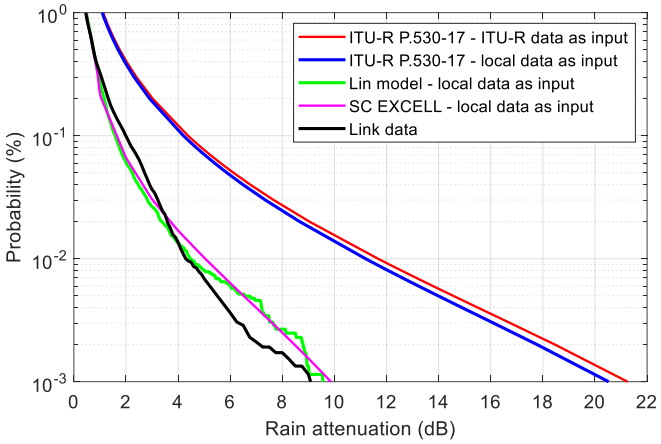

Fig. 21. Comparison between the rain attenuation CCDF measured using the link and estimated by prediction models; f = 83 GHz.

While the ITU-R model yields a strong overestimation of A'_R for both frequencies, other models providing a higher prediction accuracy are considered in the testing activity. The magenta curve in Fig. 20 and Fig. 21, which is in good agreement with the measurements, is obtained by applying the SC EXCELL model for terrestrial link [6]. The model is the adaptation to terrestrial links of SC EXCELL, which was initially conceived to estimate rain attenuation statistics affecting Earth-space links [25]. The prediction methodology relies on simulating the interaction between the electromagnetic link and various exponentially-shaped rain cells. The probability of occurrence of each rain cell, uniquely identified by its peak rain rate R_M and its effective dimension ρ_0, is a function of the input rain rate CCDF [6].

0018-926X (c) 2019 IEEE. Personal use is permitted, but republication/redistribution requires IEEE permission. See http://www.ieee.org/publications_standards/publications/rights/index.html for more information.

This article has been accepted for publication in a future issue of this journal, but has not been fully edited. Content may change prior to final publication. Citation information: DOI 10.1109/TAP.2019.2957116, IEEE Transactions on Antennas and Propagation

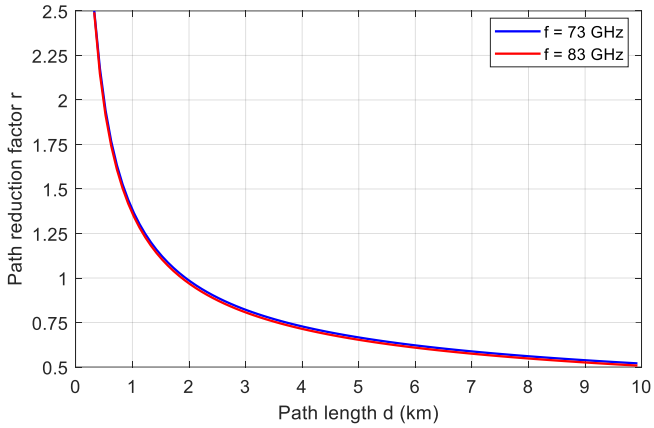

Fig. 22. Path reduction factor r in recommendation ITU-R P.530-17 as a function of the link path length d (ITU-R derived inputs).

Accurate results are achieved also by using the model proposed by Lin in [7], whose predictions are represented by the green curves in Fig. 20 and Fig. 21. Similarly to the ITU-R model, the Lin model still relies on the concept of path reduction factor, which, however, has a much simpler expression [7]:

$$r = \frac{1}{1 + d/d_R} \tag{12}$$

where d (km) is the path length in km, and d_R (km) is calculated as:

$$d_R = \frac{2636}{R(P) - 6.2} \tag{13}$$

In (13), $R(P)$ (mm/h) is the rain rate exceeded for P% of the yearly time. Finally, the path attenuation exceeded for P% of the yearly time is calculated as:

$$A(P) = k \cdot R(P)^{\alpha} \cdot d \cdot r \tag{14}$$

As is clear from Fig. 20 and Fig. 21, both the SC EXCELL and Lin models provide accurate predictions. The advantage of the former is its sound physical basis, which increases its reliability and applicability to a wide range of frequencies without the need to tune any coefficient of the model; on the other hand, the SC EXCELL model is not of straightforward application, at least not as much as the Lin model. This is indeed a key advantage of such a model, which, on the other hand, being of empirical nature, is likely to be of more limited applicability if compared to SC EXCELL: though it was not tested on longer links and different frequencies (which is out of the scope of this paper), nevertheless, the Lin's model is expected to provide accurate predictions for short links regardless of the operational frequency (as already shown for optical wavelengths [26]): in fact, the path reduction factor does not depend on the frequency, whose effect is expressed only through k and α in (14). Finally, it is worth noticing that the increased accuracy of both SC EXCELL and the Lin model is partially ascribable to the fact that they receive as input the full rain rate CCDF, while, on the contrary, the ITU-R model makes use only of $R_{0.01\%}$.

VII. Conclusions

This contribution presents the results on a joint research activity carried out by Politecnico di Milano and Huawei aimed at exploring the use of E-band terrestrial links as part of 5G mobile networks. Specifically, the research activity aimed at investigating the attenuation due to rain, A_R, which was derived from the received power level by means of a novel approach that relies on using as reference the attenuation due to gases, as well as by taking advantage of the rain events measured by the collocated radiometer. Such data were also exploited to investigate and remove the portion of the attenuation due to the wet antenna effect by means of a simple yet effective model. Results have clearly shown the marked dependence of A_R on the drop size distribution, which increases more and more with the frequency: especially for very intense events (rain rate R higher than 50 mm/h), A_R as estimated from DSD data is in good agreement with the measurements, while the use of ITU-R P.838-3, i.e. of a specific attenuation independent of the DSD, leads to overestimation. The in-depth investigation of the most intense rain events has pointed out that during convective downpours, the rain rate is not homogeneous along the path, even in the case of links as short the ones considered in this work: in turn, this is a clear hint that the path reduction factor, employed in several prediction models to take into account the spatial variability of the rain rate, is lower than 1. This is the main reason of the strong overestimation shown in the testing activity by the statistical prediction model currently recommended for terrestrial links by the ITU-R (P.530-17): for links whose path length is shorter than 2 km, the path reduction factor steeply increases beyond 1. On the other hand, a much better accuracy was found by testing the SC EXCELL model and the Lin model, which, in fact, turn out to represent much better options than the in-force ITU-R model to estimate rain attenuation on EHF short terrestrial links (d < 2 km). Although additional experimental data are needed to corroborate these conclusions, results indicate that the ITU-R model needs to be improved in order to be applicable for the prediction of rain attenuation along the short high-frequency terrestrial links that will contribute to enabling 5G mobile systems in the near future.

Acknowledgment

The authors thank NASA for making disdrometric data available.

References

[1] T. S. Rappaport, R. W. Heath Jr, R. C. Daniels, J. N. Murdock, "Millimeter wave wireless communications," Pearson Education, 2014.

[2] T. S. Rappaport, S. Sun, R. Mayzus, H. Zhao, Y. Azar, K. Wang, G. N. Wong, J. K. Schulz, M. Samimi, F. Gutierrez, "Millimeter Wave Mobile Communications for 5G Cellular: It Will Work!," *IEEE Access*, vol. 1, pp. 335–49, May 2013.

[3] A. Paraboni, C. Riva, L. Valbonesi, M. Mauri, "Eight Years of ITALSAT Copolar Attenuation Statistics at Spino d'Adda," *Space Communications*, vol. 18, no. 1-2, pp. 59-64, 2002.

[4] Propagation data and prediction methods required for the design of terrestrial line-of-sight systems. Geneva, ITU-R recommendation P.530-17, 2017.

[5] L. da Silva Mello and M. S. Pontes, "Unified method for the prediction of rain attenuation in satellite and terrestrial links," *Journal of Microwaves,*

0018-926X (c) 2019 IEEE. Personal use is permitted, but republication/redistribution requires IEEE permission. See http://www.ieee.org/publications_standards/publications/rights/index.html for more information.

This article has been accepted for publication in a future issue of this journal, but has not been fully edited. Content may change prior to final publication. Citation information: DOI 10.1109/TAP.2019.2957116, IEEE Transactions on Antennas and Propagation

Optoelectronics and Electromagnetic Applications, vol. 11, no. 1, June 2012.

[6] L. Luini, C. Capsoni: "The SC EXCELL model for the prediction of rain attenuation on terrestrial radio links," *Electronics Letters*, Vol. 49, Issue 4, pp. 307-308, 14 February 2013.

[7] S.H. Lin, "A method for calculating rain attenuation distributions on microwave paths," *Bell System Techology Journal*, pp. 1051-1086, 1975.

[8] F. Moupfouma, "Improvement of a rain attenuation prediction method for terrestrial microwave links," *IEEE Transactions on Antennas and Propagation*, vol. 32, pp. 1368-1372, 1984.

[9] L. Luini, G. Roveda, M. Zaffaroni, M. Costa and C. Riva, "EM wave propagation experiment at E band and D band for 5G wireless systems: Preliminary results," *12th European Conference on Antennas and Propagation (EuCAP 2018)*, London, 2018, pp. 1-5.

[10] Thies Clima Laser Precipitation Monitor: Instructions for Use. Rev. 2.5. July 2011.

[11] T. Rossi, M. De Sanctis, M. Ruggieri, C. Riva, L. Luini, G. Codispoti, E. Russo, G. Parca, "Satellite Communication and Propagation Experiments Through the Alphasat Q/V Band Aldo Paraboni Technology Demonstration Payload," *IEEE Aerospace and Electronic Systems Magazine*, vol. 31, no. 3, pp. 18 – 27, March 2016.

[12] Attenuation by atmospheric gase. Geneva, ITU-R recommendation P.676-11, 2016.

[13] L. Luini, C. Riva, "A Simplified Model to Predict Oxygen Attenuation on Earth-space Links," *IEEE Transactions on Antennas and Propagation*, vol. 65, no. 12, pp. 7217-7223, December 2017.

[14] L. Luini, C. Riva, "Improving the Accuracy in Predicting Water Vapor Attenuation at Millimeter-wave for Earth-space Applications," *IEEE Transactions on Antennas and Propagation*, vol. 64, no. 6, pp. 2487-2493, June 2016.

[15] X. Boulanger, B. Gabard, L. Casadebaig and L. Castanet, "Four Years of Total Attenuation Statistics of Earth-Space Propagation Experiments at Ka-Band in Toulouse," *IEEE Transactions on Antennas and Propagation*, vol. 63, no. 5, pp. 2203-2214, May 2015.

[16] J. M. Riera, G. A. Siles, P. Garcia-del-Pino and A. Benarroch, "Alphasat propagation experiment in Madrid: Processing of the first year of measurements," 2016 *10th European Conference on Antennas and Propagation (EuCAP)*, Davos, 2016, pp. 1-5.

[17] Specific attenuation model for rain for use in prediction methods. Geneva, ITU-R recommendation P.838-3, 2005.

[18] H.Y. Lam, L. Luini, J. Din, C. Capsoni, A. D. Panagopoulos, "Investigation of Rain Attenuation in Equatorial Kuala Lumpur," *IEEE Antennas and Wireless Propagation Letters*, vol. 11, pp. 1002-1005, 2012.

[19] M. Sadiku, Numerical Techniques in Electromagnetics, 2nd Ed., CRC Press, 2001.

[20] M. Mishchenko, L. Travis, A. Lacis, "Scattering, Absorption, and Emission of Light by Small Particles," Cambridge University, 2002.

[21] K. Beard, C. Chuang, "A New Model for the Equilibrium Shape of Raindrops," *Journal of the Atmospheric Sciences*, vol. 44, no. 11, pp. 1509-1524, 1987.

[22] E. S. Hong, S. Lane, D. Murrell, N. Tarasenko and C. Christodoulou, "Mitigation of Reflector Dish Wet Antenna Effect at 72 and 84 GHz," *IEEE Antennas and Wireless Propagation Letters*, vol. 16, pp. 3100-3103, 2017 (doi: 10.1109/LAWP.2017.2762519).

[23] M. M. Z. Kharadly, Robert Ross, "Effect of Wet Antenna Attenuation on Propagation Data Statistics," *IEEE Transactions on Antennas and Propagation*, vol. 49, no. 8, pp. 1183-1191, August 2001.

[24] J. M. Garcia-Rubia, J. M. Riera, P. Garcia-del-Pino, A. Benarroch, "Attenuation Measurements and Propagation Modeling in the W-Band," *IEEE Transactions on Antennas and Propagation*, vol. 61, no. 4, pp. 1860-1867, April 2013

[25] C. Capsoni, L. Luini, A. Paraboni, C. Riva, A. Martellucci, "A new prediction model of rain attenuation that separately accounts for stratiform and convective rain," *IEEE Transactions on Antennas and Propagation*, Vol 57, No. 1, January 2009, Page(s): 196 - 204.

[26] U. A. Korai, L. Luini, R. Nebuloni, "Model for the Prediction of Rain Attenuation Affecting Free Space Optical Links," *Electronics 2018*, 7(12), 407, pp. 1-14, December 2018.

0018-926X (c) 2019 IEEE. Personal use is permitted, but republication/redistribution requires IEEE permission. See http://www.ieee.org/publications_standards/publications/rights/index.html for more information.